



# Explosive Weapons and ARMs Detection with Singular Classification (WARDIC) on novel Weapon Dataset using Deep Learning: Enhanced OODA (Observe, Orient, Decide, and Act) Loop

Anant Bhatt<sup>\*,#</sup> and Amit Ganatra<sup>#</sup>

## Abstract

Rising armed conflicts and violent agitations in populated areas have upstretched stark trepidations worldwide. Especially, the armed conflicts are increasingly being fought using explosive weapons, rifles, and lethal arms, endangering civilian lives and infrastructure. Concerns raised by the state actors accentuate the importance of identifying the miscreants possessing explosive weapons to limit unlawful activities. Armed forces, and law enforcement agencies, while carrying out operations in populated areas, demand the high availability of meaningful information promptly to shorten the OODA (Observe, Orient, Decide, and Act) loop for effective decision-making by the military commanders. Existing research is limited to classifying revolvers, pistols, and knives. It has privations to detect explosive weapons and firearms due to the severe void of relevant datasets and computationally optimal weapon detection methodology, which imposes severe restrictions in instrumenting an effective system. Hence, we introduce two customized, high-balanced Novel Operational Weapon Arms Datasets - named NOWAD post detailed Exploratory Data analysis. We propose a state-of-the-Art methodology to implement a novel weapons and arms detection singular classifier -named (WARDIC) to identify explosive weapons and arms. The WARDIC - an augmented architecture of the ConvNets and Singular Classifiers showed promising performance in detecting weapons in surveillance feeds. The evaluation metrics show promising performance of the tuned WARDIC classifier (fusion of DenseNet-121 with the Isolation Forest) over traditional baselines models with perfect scores of 100%. Cross validations of the classifier employing 5-Fold and 10-Fold CV showed accuracy scores of 99.27% and 99.46%, respectively, with linear complexity. Our experiments propose the State-of-the-Art Classifier formulation, which shortens the OODA loop for effective decision-making by significantly improving computational complexity to instrument a quick response system. The WARDIC classifier distinctively supersedes the performance of the existing classifiers with enhanced computational speed for veristic operational scenarios.

*Keywords:* Explosive weapons & arms detection; Isolation forest; Weapon detection with CNN; Weapon detection with Transfer learning; Weapon dataset; Single class classifier; Weapon detection using Deep learning.

Received: 25 March 2022; Revised: 22 May 2022; Accepted: 24 May 2022.

Article type: Research article.

## 1. Introduction

A spurt increase in violent incidents has upstretched stark trepidations in various countries where explosive weapons and small arms are being used against legitimate targets located in populated areas. According to the United Nations official, nearly 250,000 deaths occur every year due to gun (or small

weapons) violence.<sup>[1]</sup> On another end, armed conflicts are increasingly being fought using explosive weapons, rifles, and lethal small arms in populated areas, involving armed forces, law enforcement agencies, and civilians. Certain cases of conflict worldwide highlight armed conflict led by insurgency, the rise of terrorist activities, and civil wars/ agitations with weapons and arms. Such unlawful occurrences by miscreants led to incidental (collateral) effects on civilians and civilian objects. The humanitarian concerns arising from using explosive weapons and arms in populated areas include the conspicuous impact on civilian lives, mental well-being, civilians' health, physical disabilities, and civilian

*Devang Patel Institute of Advance Technology and Research, Charotar University of Science and Technology, Nadiad Petlad Road, Changa, 388421, Gujarat, India.*

<sup>#</sup> These authors contributed to this work equally.

\*E-mail: [capt.anant@gmail.com](mailto:capt.anant@gmail.com) (A. Bhatt)

infrastructure.<sup>[2]</sup>

The vulnerability of critical government, military and belligerents, and non-State armed groups, often avoid facing their opponents in direct conflict in the open, intermingling instead with the civilian population.<sup>[3]</sup> Escalation of any violence using arms and explosive weapons in civilian or populated areas may trigger intense conflicts and even civil wars. A high chance of a rise in such conflicts in the future is envisaged, thereby exposing civilians to further risk of harm. Fig. 1 shows images from violent agitations, clashes, and armed conflicts in the populated civil areas where groups of people have been using explosive weapons and arms, as reported by news agencies.<sup>[4-9]</sup> Concerns raised by the state actors and law enforcement agencies accentuate the importance of planning operations in populated areas to thwart such incidents. An immediate requirement highlights the identification of the miscreants in possession of explosive weapons and limits unlawful activities. Proposed work is preceded by studying all available work on the subject. However, these studies are found to be preliminary research in detecting personal weapons that only detect pistols or revolvers.

The military and law enforcement operation in populated areas demands the high availability of meaningful information for timely actions. The ability to extract, process, and access information on the location contribute to the forces' agility. However, imprecise situational awareness, human inaccuracies in information compilation, chaotic information flow, and constricted reaction time may lead to nonconformity of rational thinking and result in a decision dilemma. OODA (Observe, Orient, Decide, and Act), developed by strategist and United States Air Force Colonel John Boyd, is a widely used model in the decision-making process by many military/law enforcement agencies during the conduct of military

civilian infrastructure also poses severe concerns by the state authorities. The majority of reported clashes bring out that operations.<sup>[10]</sup> The OODA model extends a practical concept called the OODA loop, designed to underpin rational thinking in muddled situations. An effective OODA loop empowers the commanders in the decision-making process.<sup>[11-13]</sup> The OODA loop incorporated four interrelated, smaller loops: observe, orient, decide, and act, encouraging decision-makers to think critically, anticipate threats, and neutralize them before becoming critical. We deliberated on technical and methodological challenges in identifying visual features and explosive weapons and arms patterns, which pose restraints in prompt detection. We evaluated various OODA loops modifications for various operational scenarios based on the technical and operational voids. With the advent of disruptive technologies, *i.e.*, Deep Learning and high computation-powered computers, the edge devices in surveillance systems are getting smarter. These intelligent devices can be implanted with intelligence to aid such operations. We propose a novel and Artificial Intelligence-driven conceptualized OODA model which shortens the OODA loop (as illustrated in Fig. 2) by prompt detection of explosive weapons arms, extraction, and aid analyses of relevant information to prevent incidental civilian harm.

The subsequent paragraphs use 'Explosive Weapon and Arms' with 'Small Arms' interchangeably to convey the same meaning used in the military context. The lack of relevant datasets with maximum chromatic exposure and a variety of weapons encountered in armed conflicts restricts the development of concrete methodology. The paper proposes an innovative methodology to implement a novel Singular Explosive Weapons and Arms Detection using an isolation Classifier (WARDIC) to introduce our customized, high-balanced Novel Operational Weapon Arms Dataset (NOWAD).



**Fig. 1** Violent agitations, clashes, and armed conflicts in populated civil areas where explosive weapons and arms are being used, as reported by various news agencies.

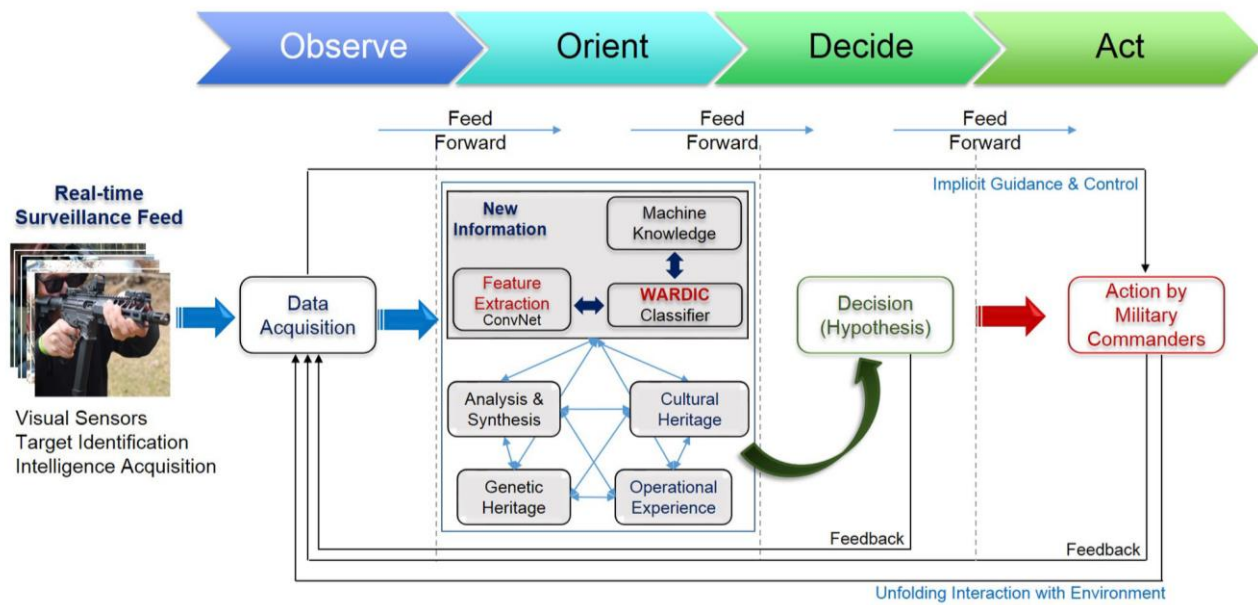


Fig. 2 Modified OODA loop -re-conceptualized based on J. R Boyd proposed OODA loop.

The proposed novel employment model shortens the OODA loop by prompt detection of explosive weapons/ arms, extraction, and aid analyses of relevant information to prevent incidental civilian harm. The proposed work contributes as follows:

- The work introduces highly relevant, balanced explosive and firearms weapon datasets- named Novel Operational Weapon Arms Dataset (NOWAD) with a wide diversity of explosive weapons and small arms models and makes with visual exposures akin to operational situations.
- The approach presents an innovative methodology to implement a novel Singular Explosive Weapons and Arms Detection using the isolation Classifier (WARDIC).
- The work also proposes an enhanced hybrid architecture by exploiting ConvNet for feature extraction and One-Class SVM or Isolation Forest for classification, demonstrating promising results over the Baseline ConvNet models when applied with the Transfer Learning technique.
- The conclusive study demonstrates a comparative analysis of the results generated by amalgamated models/ techniques.

The proposed work is preempted by a detailed literature analysis on the subject. Most of the published work mentioned in Table 1 proposes a binary or three-class classification for detecting and classifying personal weapons, *i.e.*, pistols, knives, revolvers, and handguns. Almost every work uses open-source images, web scrapped from the internet, or local CCTV camera video conversions. There is no availability of a standard dataset. Using the customized / hybrid dataset may lead to conspicuous results but cannot be compared on the standard scale. We highlight that there is no work done on detecting firearms and lethal weapons detection. The above works target detecting and classifying objects that can

empower the security arrangements that can help in scenarios like robbery, loot, or civil crimes. The experiments in the referenced works of literature are carried out on datasets that are skewed, unbalanced, and short of the mark. During the literature review, proposed models and combination approaches were analyzed by studying their performance scores and highlighted that these methodologies demand computationally heavy infrastructure, unsuitable for actual operations for speedier detections. Though the Convolution Neural Networks (CNN) can generate a significant solution to the classification problems, the lack of relevant dataset and computational cost imposes severe restrictions on instrumenting a functional system. Vallez N et al. highlight the work to optimize classification performances using auto-encoders post object detection.<sup>[14]</sup> However, there is a substantial scope to improve the CNN results to set a benchmark performance. Hence, the work was focused on effective feature extraction followed by classification to establish benchmark scores. It is emphasized that none of the experiments are intended to detect explosives and firearms for armed conflict or clashes during the operational scenario, mainly due to the non-availability of explosive arms and weapons datasets. The work is concluded by highlighting the literature study by underlining that the present research has privations of a befitting methodology for rapid identification of explosive weapons and firearms for armed conflict scenarios.

## 2. Materials

### 2.1 Dataset

The problem definition involved tangible inputs from ground operational situations while discussing with military commanders at various levels. Collecting, processing, and annotating the images required to form a dataset for the deep

**Table 1.** Essential aspects of the existing literature proposed for detecting and classifying the Weapons with various approaches.

Literature	Object Type	Image Set	Scenario	Class	CNN and Algo	Acc%
(Bhatti <i>et al.</i> , 2021) <sup>[15]</sup>	Pistol	8327	CCTV Security	Binary	VGG16, Inception-V3, InceptionResnet V2, Faster-RCNN, SSDMobileNetV1, FRIRv2, YOLOv3/v4	91.73
(Dwivedi <i>et al.</i> , 2019) <sup>[16]</sup>	Knife,Gun, Noweapon	Not Available	Proof of Concept	3	VGG-16, CNN	98.41
(Jain <i>et al.</i> , 2020) <sup>[17]</sup>	Pistol, Small Arms	1059	Proof of Concept	5	SSD, Fast RCNN	73.8
(Lai and Maples, 2017) <sup>[18]</sup>	Pistol	2753	Proof of Concept	2	VGG-16	58.0
(Narejo <i>et al.</i> , 2021) <sup>[19]</sup>	Pistol	Not Disclosed	Proof of Concept	Not Disclosed	VGG-16, YOLOv3 Fast RCNN	Requires Clarity
(de Azevedo Kane-hisa and de Almeida Neto, 2019) <sup>[20]</sup>	IMFDB	6585	Proof of Concept	Binary	YOLO	96.26
(Olmos <i>et al.</i> , 2018) <sup>[21]</sup>	Pistol, Mixed Bag	-	Proof of Concept	Binary, Multiclass	Faster RCNN, VGG-16	84.21
(Verma and Dhillon, 2017) <sup>[22]</sup>	IMFDB	-	Proof of Concept	Multiclass	VGG16, SVM, KNN, CNN	93.1
(RuizSantaquiteria <i>et al.</i> , 2021) <sup>[23]</sup>	Handguns, Pistol	3900	Proof of Concept	Pose Detection, Binary	YOLOv3, HRC	97.33

(Abbreviations: CNN-Convolution Neural Network, SVM- Support Vector Machine, VGG- Visual Geometry Group, R-CNN - Region-Based Convolution Neural Networks, HRC-Hand Region Classifier, IMFDB- Internet Movie Firearms Database, YOLO- You only look once, and Acc-Accuracy).

learning models is a time-consuming, significant task demanding considerable effort. Annotations for multiple objects with full, partial, or minuscule chromatics exposure in images require due diligence as the annotators have to select the multiple objects area within the images within which the object is located and the category. The possibility to use of public dataset was explored, but due to the non-availability of the dataset with lethal firearms, we built our datasets. We generated a customized dataset from open-source images by screening the images based on the type/ make of explosive weapons and arms used in present conflicts with adequate variety and distinction of weapon inventory. This dataset repository was filtered manually based on their image resolution, visual clarity, arms exposure, and significance to the realistic scenarios. The initial image repository contained 8300+ images collected from open sources carefully with visual exposure of the lethal Firearms only, *i.e.*, rifle, RPGs, automatic machine guns, and automatic weapons. The image scrutiny process excluded images with exposures of the weapons used in civil crimes. Fig. 3 shows dataset samples with an exposure of explosive weapons and firearms for the 'Small Arms' Class post manual filtering and detailed scrutiny, considering actual conflict and clashes.

'Openlabelling',<sup>[24]</sup> an open-source project was used to annotate the weapons in the images with singular class

annotations, labeled 'Small Arms' in one dataset and with binary class annotation (classes named- 'Small Arms' and 'Person') in the second dataset. The dataset aims to facilitate further research where overlapping bounding boxes for persons and arms are seen in real-time images, and hence, these two classes have been chosen. It was observed that weapon exposure is a crucial aspect while formulating the dataset. Hence, the process was deliberated by creating a repository of various weapons with various exposure visuals, ensuring a balanced quantity to extract weapon features, and eliminating repetitive or irrelevant viewing angles. We included most of the weapons models/ makes by incorporating images of approximately 40-60 different weapons. Fig. 4 illustrates distinctive explosive weapon perspectives to generalize the features encountered in operational scenarios effectively. Considering the weapons exposures, we carefully screened the images manually, followed by a deliberate Exploratory Data Analysis.

### 2.2 Data pre-processing

To standardize the images for the experiments, we carried out data pre-processing of 8327 images followed by Exploratory data analysis to understand the dataset characteristics. During pre-processing, batches of 500 images were formed with their respective YOLO/darknet and PASCAL/VOC files in separate



**Fig. 3** Veristic images as encountered by the Armed forces in operational scenario. The images are part of our introduced dataset-named Novel Operational Weapon Arms Dataset (NOWAD).

folders. Initial iteration encompassed image resolution identification to incorporate images with the desired resolution, *i.e.*, very high and low-resolution images falling as outliers were down-sampled/ eliminated. Region of Interest (ROI) for each object in an image was curled out using YOLO/darknet annotation files and stored in separated files. We analyzed the resulting resolution and plotted it along with their respective mean. These steps helped segregate files with objects of poor features (minimal object ROI). A noise removal filter was applied to the images by extracting the Region of Interest (ROIs) from low-resolution images, *i.e.*, Weapons/arms. The processed dataset encompassed 5828 images post-employment of noise removal filter, considering the threshold of 224.

### 2.3 Exploratory data analysis

Exploratory data analysis (EDA) is an efficient approach that facilitates highlighting the insights of the data using descriptive statistics and graphical tools. EDA helps enhance data assimilation, detect outliers and anomalies, and test underlying assumptions. EDA is a robust preliminary step before the conception of the experiments and application that helps understand the data distribution, obtain average characteristics, and, hence, subdivide or distribute if required. We deliberated on an EDA while creating the customized dataset, which performed investigations on data to identify and highlight patterns. This phase incorporated summary statistics and graphical representations to highlight salient characteristics of the dataset, and data patterns for enhanced



**Fig. 4** Weapon images with heterogeneity in the chromatic exposure of the explosive weapons and arms with distinctive viewing angles, suitable to create meaningful diversity to generalize the weapons' features from the NOWAD.

feature assimilation for images in subsequent paragraphs. The EDA graphs show that the dataset is a balanced quality dataset and can be considered the standard dataset. The average image resolution threshold was identified as 358x517 pixels for our datasets during the analysis. Based on the inferences curled from ImageNet challenges.<sup>[25,26]</sup> Fig. 5 shows the average image dimensions are 385x517 pixels in our dataset, ensuring that a significant portion of the information is retained in the dataset post-filtration. The final dataset comprised 4662 images in training set with an appropriate variety of weapons.

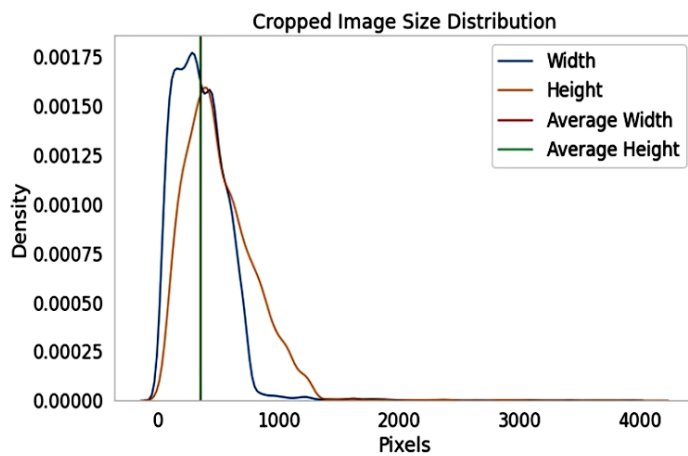


Fig. 5 Density distribution of the dimensions of images from the raw corpus (prior formulation of the NOWAD).

During the process, the images were chosen, which ensure adequate diversity (object visual exposure), ensure adequate weapons' feature variety, remove outlier images, and reduce similar weapon exposure to standardize the objects for effective machine learning in subsequent steps. We initiated an analysis of the filtered dataset for weapons' features which produced approximately 5000 features. Incorporating all features in subsequent experimental steps will incur a high probability of a biased model since most of the extracted feature values were null. Principal component analysis (PCA) was used that can analyze the dataset considering inter-

correlated quantitative dependent variables. PCA - a multivariate technique was used to extract the vital information of the objects and represent them in heterogeneous sets of orthogonal variables called Principal Components<sup>[27]</sup>, which eliminated the possibility of biases by reducing the feature count to 1/10th of the original size. Fig. 6 shows the Principal Component values (not dominated by zeroes), highlighting information-rich dense vectors of (all images) in a heatmap for (a) Training set and (b) Testing set. To ascertain the distribution of the components, we presented the image features' values in a joint plot where each vertical line (with data points) represents each image. Fig. 7 shows the uniform data distribution (in a margin area with a wide, feeble white colored band) at the center, implying the absence of outliers. Fig. 8 shows a weak correlation (with a correlation index value of less than 0.4) among the newly extracted features on a heatmap for the training dataset, implying that the feature set incorporates unique, relevant features. During the iterative EDA, we spotted the anomalies using Figs. 6-8, removed irrelevant features, and concise the dataset after deliberate test hypotheses. The proposed NOWAD dataset is the balanced dataset, which incorporates adequate, unique images to meet the operational requirements. We split the dataset into a standard ratio of 80:20 for the training and testing phases.

2. Methods and experimental section

The research incorporates the experiments with concentrated efforts to address the problem statement by creating a relevant dataset and proposing a novel methodology of uni-class classifier - Weapons and Arms Detection using isolation Classifier (WARDIC). 'WARDIC' is a novel methodology of augmenting the ConvNets for their feature extraction capability and then carrying out uni-class classification using linear-complexity techniques. The work proposes to use CNNs as 'Feature Extractor' models to extract the features from the NOWAD images. We used numerous ConvNet models, i.e., VGG-16, VGG19,<sup>[28]</sup> MobileNetV2,<sup>[29]</sup> MobileNet,<sup>[30]</sup>

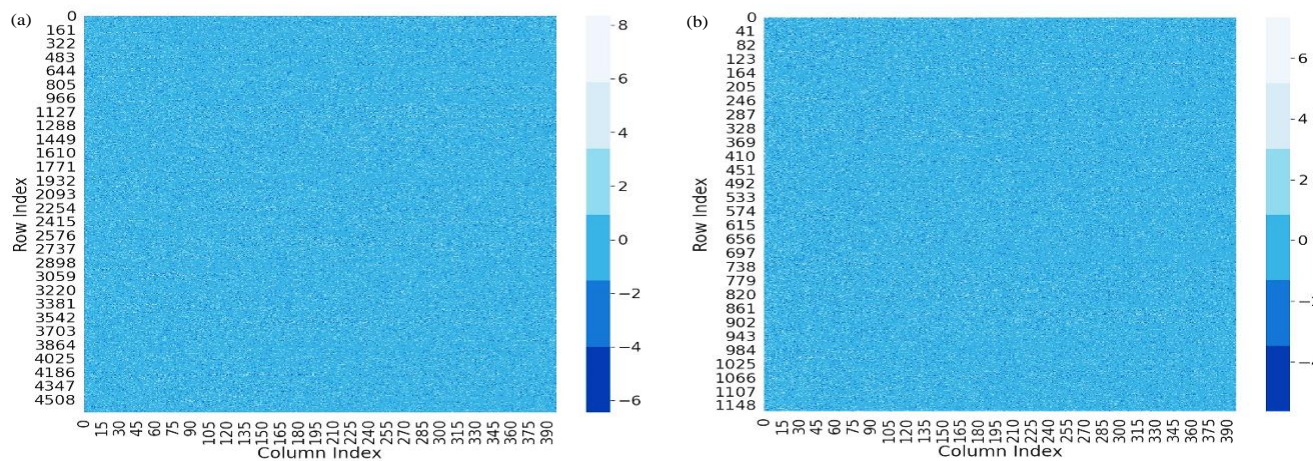
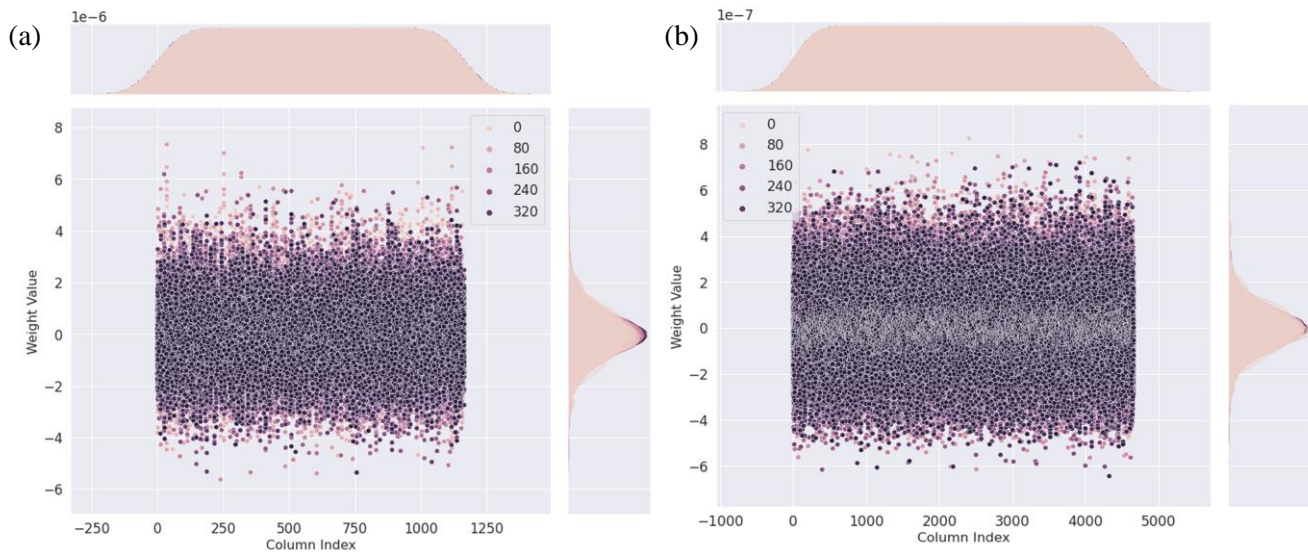


Fig. 6 The component values (not dominated by zeroes) on a heatmap of the Dataset splits, i.e., (a) Training Dataset, (b) Testing Dataset, highlighting that the features represent an information-rich dense vector.



**Fig. 7** Joint plot of value distribution of the dataset, *i.e.*, (a) Training dataset, (b) Testing dataset. The plot at (b) highlights a uniform data distribution in a margin with a wide, feeble white colored band (near zeroes) at the center of the joint plot, which implies the absence of outliers.

InceptionV3,<sup>[31]</sup> InceptionResNetV2, DenseNet121,<sup>[32]</sup> EfficientNetB0, EfficientNetB1<sup>[33]</sup> and, NASNetMobile<sup>[34]</sup> models with pre-trained weights from the ImageNet dataset, referred to as Transfer Learning<sup>[35]</sup> due to its promising yields.<sup>[36,37]</sup> Performance of these CNNs are compared on the evaluation carried out on ImageNet dataset in the [Table 2](#).

As pre-trained ConvNets involve considerable time to train across multiple GPUs for the sizeable dataset, Transfer Learning can reduce the training time with effective outcomes. Since exploratory data analysis of the NOWAD highlights that the scope of the target dataset collides with the source dataset (ImageNet dataset), the pre-trained models can yield improvised outcomes with curtailed training overheads. A labeled source dataset and a labeled target dataset were used during the training of the models. Fixed feature extractor

approach was implemented on various ConvNets (pre-trained on the ImageNet dataset). While conceiving the experiments, we chose the pre-trained model, considering a correlation and knowledge compatibility between the ImageNet dataset knowledge (of the pre-trained source model) and the NOWAD weapon detection domain. Base models were created by shedding classifier layers of the models where the last fully-connected layer were detached and explored the ConvNet as a fixed feature extractor for the target dataset. The approach benefits in avoiding overfitting on NOWAD as it objected to retraining the classifier only by freezing the Convolutional Base.

The calculated parameters were accessed at the max-pooling layer, which acts as an Image Representation Vector or Image Features by removing fully connected layers from

**Table 2.** Comparative study of performances of ConvNets models, *i.e.*, VGG16, VGG-19, MobileNet, MobileNetV2, InceptionResNetV2, DenseNet121, EfficientNet B0, EfficientNet B1, and NASNetMobile. The comparative numbers highlight Model's size; top-1 / top-5 accuracy (on the ImageNet validation dataset), Params, Depth (number of layers with parameters), and inference time/ step on CPU (AMD EPYC Processor (with IBPB) (92 core), RAM-1.7T), and GPU (Tesla A100, Batch size: 32).

ConvNet	Size (MB)	Top-1 Acc	Top-5 Acc	Params	Depth	Time (ms) per inference step (CPU)	Time (ms) per inference step (GPU)
VGG-16	528	71.3%	90.1%	138.4M	16	69.5	4.2
VGG-19	549	71.3%	90.0%	143.7M	19	84.8	4.4
MobileNet	16	70.4%	89.5%	4.3M	55	22.6	3.4
MobileNet V2	14	71.3%	90.1%	3.5M	105	25.9	3.8
Inception ResNetV2	215	80.3%	95.3%	55.9M	449	130.2	10.0
DenseNet121	33	75.0%	92.3%	8.1M	242	77.1	5.4
EfficientNetB0	29	77.1%	93.3%	5.3M	132	46.0	4.9
EfficientNetB1	31	79.1%	94.4%	7.9M	186	60.2	5.6
NASNetMobile	23	74.4%	91.9%	5.3M	389	27.0	6.7

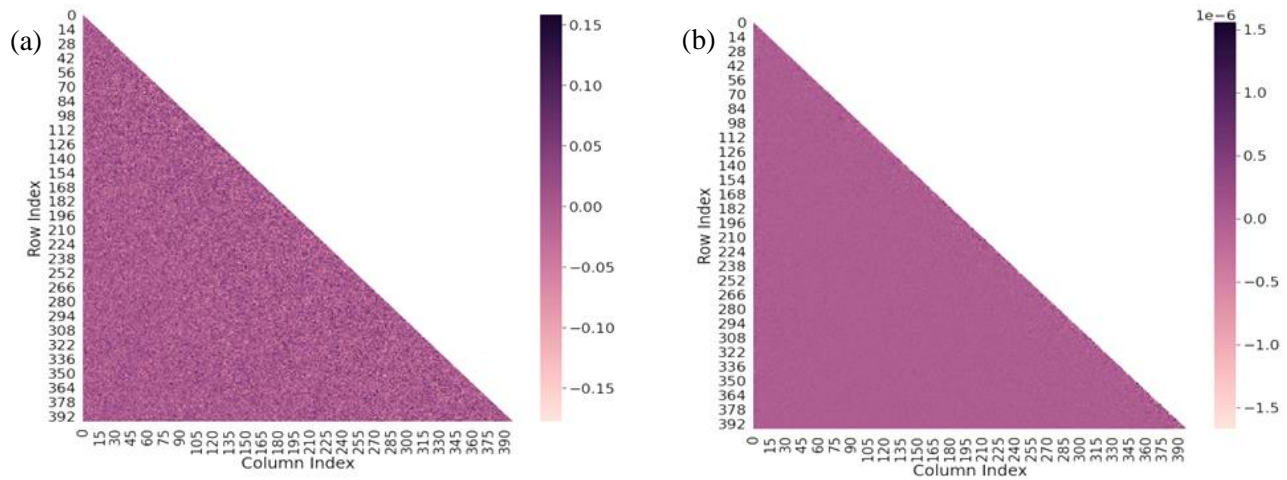


**Fig. 8** Heatmap of correlation of feature sets in (a) Training Dataset, (b) Testing Dataset. The plot highlights a weak correlation (with a correlation index value of less than 0.4) among the newly extracted features on a heatmap for the training dataset, implying that the feature set incorporates unique, relevant features.

the output layer.<sup>[38]</sup> The 'Feature Selection' was done on these extracted features, followed by feeding the selected features to the uni-class classifier, *i.e.*, One-class SVM<sup>[39]</sup> and Isolation Forest. Fig. 9 shows the implementation methodology and inference pipeline for the 'WARDIC.' There are sequential stages to designing this workflow and conducting the experiments in order (1) Model Implementation, (2) Singular Classifier Fusion, (3) Testing \& Validation.

**3.1 Model implementation: Feature extraction with convNets**

During Model implementation, VGG19, VGG16,

MobileNetV2, MobileNet, InceptionV3, InceptionResNetV2, DenseNet121, EfficientNetB0, EfficientNetB1 and NASNetMobile models were explored for feature extraction. Transfer Learning was employed by taking the pre-trained weights from the ImageNet while experimenting with various ConvNet models. For feature map extraction from our customized dataset, the output layer detached that contains fully connected layers (which generates the final output from the feature map) of these Conv Net models. The ConvNet models processed the batch of images (size of  $224 \times 224$ ) to derive feature maps wherein former layers captured the low-level features, *i.e.*, weapons/ arms boundary, partial

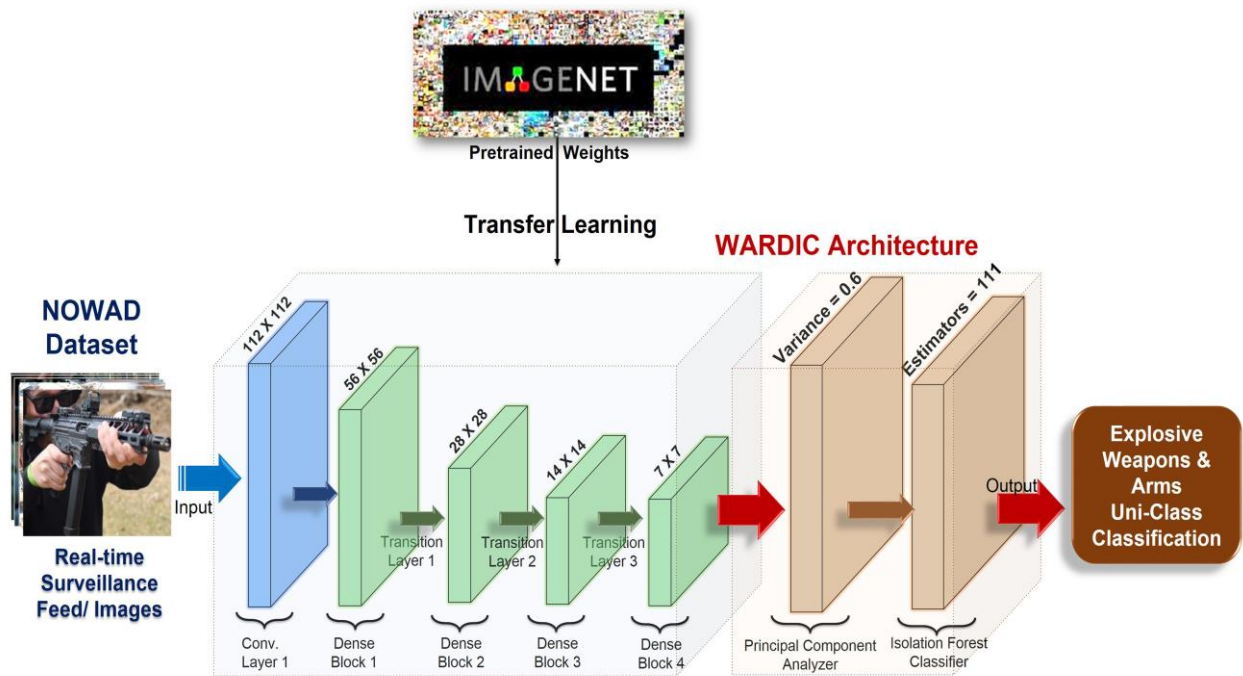


**Fig. 9** Implementation methodology and the inference pipeline with the employment of Transfer Learning Technique on ConvNets model for feature extraction followed by fusing a singular classifier to detect explosive weapons and arms from the surveillance feeds.

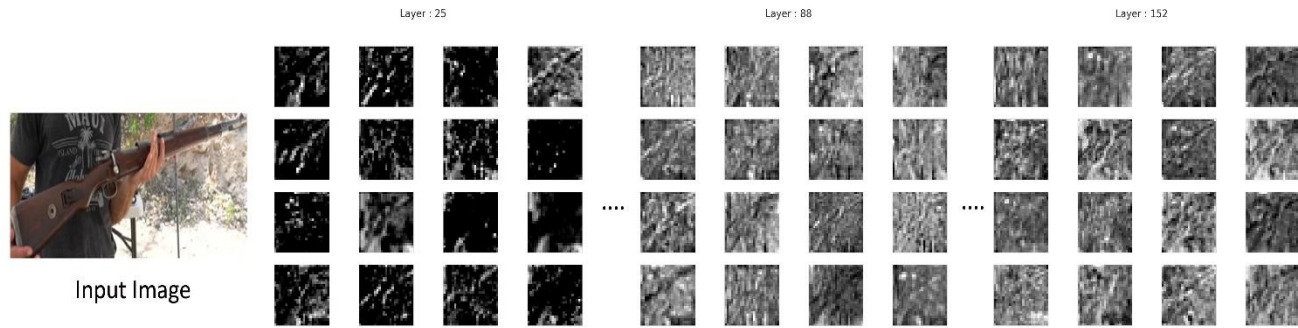


**Fig. 10** The feature extraction intermediate outputs of the DenseNet121 ConvNet layer 25, 88 and 152 wherein former layers captured the low-level features, *i.e.*, weapons/ arms boundary, partial shapes/characteristics, and later layers derived high-level features to detect the weapon.

shapes/characteristics, and later layers derived high-level features from categorizing the object based on weapons shapes, as shown in Fig. 10. The further step transformed the feature map of each image into a one-dimension vector with 25,088 features. It scaled these features by applying the transformation to each column to achieve the closest value to the unity of the standard deviation. Dataset had 5882 images with a split of 4662 images in the training set and 1166 images in the test set. The dataset dimensions were reshaped, which benefits the ConvNets models, allowing the last convolutional and classification stages to train. One-Class Support Vector Machine/Isolation Forest Classifier was employed during the last step. The experiments were conducted on the collaborative platform's Tesla K80 GPU and 11 GB RAM. Principal Component Analysis was applied to further reduce the number of features and select the relevant components. Fig. 6 shows the correlation graph for the Components vs. Variability distribution. We conduct experiments with different principal component values starting from 2 and increasing with the multiple of 2. To eliminate the possibility of overfitting in the model, we propose a variability value of approximately 0.6-0.7. Fig. 11 highlights that a further increase of variability beyond the value of 0.6 introduces a sudden rise in the total number of features, e.g., an increase of

mean variability of 0.2 doubles the number of total features, which will result in overfitting and slow prediction speed. We derived approximately 150 to 600 meaningful features for each image, as shown in Fig. 11. These features are used for classifying objects. We propose the implementation of Singular Classifier as it tends to address the problem definition. We propose experiments on two Singular Classifiers, *i.e.*, One-Class Support Vector Machine and Isolation Forest.

**3.2 Singular classification: One-class support vector machine (OCSVM)**

Several experiments of different ConvNet for feature extraction were conducted. We employed isolation forest and One-class Support Vector Machine (OCSVM) as a classifier for the features.<sup>[40]</sup> One-class SVM is an algorithm that learns a decision function for novelty detection, thus classifying new data with a hypersphere to encompass all instances.<sup>[41,42]</sup> To carry out the optimal tuning of the model, we tuned the values of  $\nu$ , where  $\nu$  is a property representing the upper bound on the fraction of outliers and enables the model to control the trade-off between outliers and normal cases. The kernel value was identified as 'rbf', gamma = 0.001, and  $\nu$  value as 0.08 after several iterative experiments.

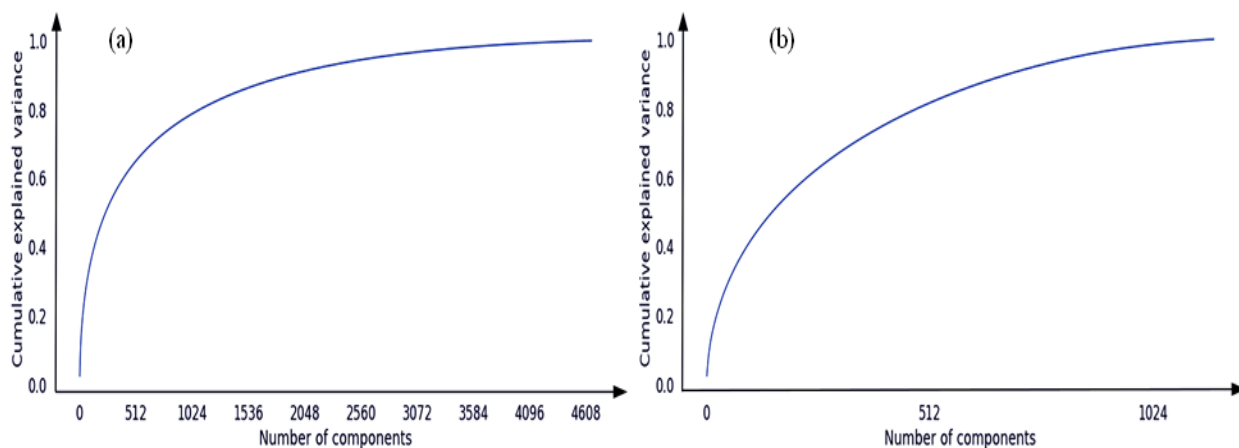


**Fig. 11** Variance distribution of features w.r.t. the number of components in PCA (a) Training Split (b) Test Split, where the higher number of features implies more information inclusive of the noise component in images.

### 3.3 Singular classification: Isolation forest

The approach used an unsupervised and nonparametric - Isolation Forest algorithm to detect anomalies with faster calculations in real-time scenarios. The algorithm detects anomalies by assigning an anomaly score  $t$ . We used an unsupervised and nonparametric - Isolation Forest algorithm to detect anomalies with faster calculations in real-time scenarios. The algorithm detects anomalies by assigning an anomaly score to the observations (per the tree depth). Since outliers will take a less-than-average number of splits to become isolated, the trees are built up corresponding to the height of a perfectly-balanced binary search tree -  $\log_2(n)$ .<sup>[43,44]</sup> The expected path length  $c(n)$  can be obtained using Formula 1.

$$C(n) = 2H_{n-1} - \frac{2^{(n-1)}}{n} \tag{1}$$

where,  $H(i)$  is the harmonic number, and estimated by  $\ln(i) + 0.5772156649$  (Euler–Mascheroni constant).  $C(n)$  is the average of path length  $h(x)$  given  $n$ ; we use it to normalize  $h(x)$ . The isolation forest algorithm composes many isolation trees (not taller than the max height) for a given dataset and performs well on sub-sampled data. The Isolation Forest has a linear time complexity (computationally expensive operations) with a low constant, making it low on memory footprint. During the training, the Isolation Forest creates numerous Isolation trees for different features using three imperative parameters named- estimators( $X$ ), samples( $n$ ), and features( $m$ ). The isolation forest generates an Anomaly Score to identify anomalous data point with values ranging between 0 and 1. The anomaly score is as shown at Formula 2.

$$s(x,n) = 2^{-E(h(x))/c(n)} \tag{2}$$

$E(h(x))$  is the average of  $h(x)$ , which is the path length from the root node to the external node  $x$ , while  $c(n)$  is the average of  $h(x)$  given 'n' and is used to normalize  $h(x)$ . An anomaly score closer to the unity indicates a smaller path length, implying the data point is an anomaly. In contrast, the score is smaller than 0.5, indicating a case is a normal data point. If all the observations have an anomaly score of around 0.5, the algorithms derive no anomaly in the entire sample. The

experiments calculated the anomaly score for each tree and averaged the score for all the isolation trees to identify the anomalies. After several iterative experiments, we finalized the contamination value as 0.08 and the estimator's value as 40. Fig. 12 shows the co-relation and accuracy score distribution while employing different values of the Number of Estimators in Isolation Forest Classifier and  $\nu$  parameter in One-Class SVM classifier, augmented with DenseNet-121. The figure help to identify the optimum values of the estimators, and the  $\nu$  is the parameter by visualizing the trade-off between overfitting and correct prediction.

A one-dimensional vector equal to rows was constructed during the subsequent step to establish the ground truth. The training set is used to fit the One-class SVM and Isolation Forest Classifier with default parameters to set the baseline for the study. The test split is constructed with all the values marked as unity. The predictions were derived for the test split with the One-class SVM and Isolation Forest Classifier, followed by a comparison with ground truth. To validate the WARDIC classifier variations after hyper parameter tuning, we used the n-fold cross-validation technique on the train and tested the split of features. The approach involved n-fold cross-validation with  $n=5$  and 10. Scores using the ConvNet model with One-class SVM and Isolation Forest Classifier were generated to evaluate the comparative performance by employing the augmented architecture and fusing with 5-fold and 10-fold cross-validations. The experiments highlight that DenseNet121 ConvNet (feature extraction model) augmented with both One-class SVM and Isolation Forest Classifier generated promising results with performance scores near to the unity for which we show the performance patterns for each fold in Fig. 13. The Accuracy Score Plot shows promising results for both the classifier's cross-validation, i.e., 5 and 10-Fold.

## 4. Results and Discussion

### 4.1 Evaluation Parameters

The WARDIC performance was evaluated based on the performance metrics, especially measuring the performance

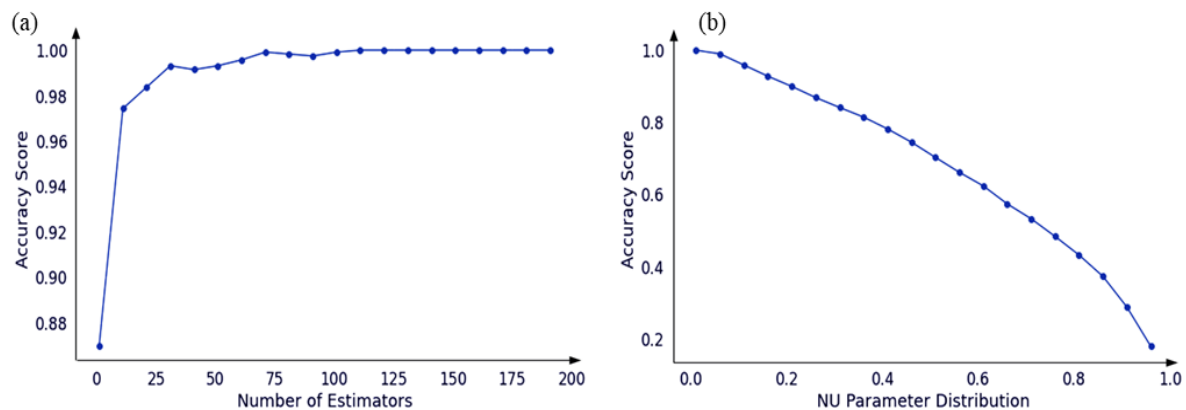


**Fig. 12** Co-relation and accuracy score distribution for (a) Number of Estimators in Isolation Forest Classifier and (b)  $\nu$  parameter in One-Class SVM classifier, augmented with DenseNet-121 (for feature extraction). The figure illustrates the optimum values of the estimators, and the  $\nu$  is the parameter for respective algorithms, comparing the trade-off between overfitting and correct prediction.

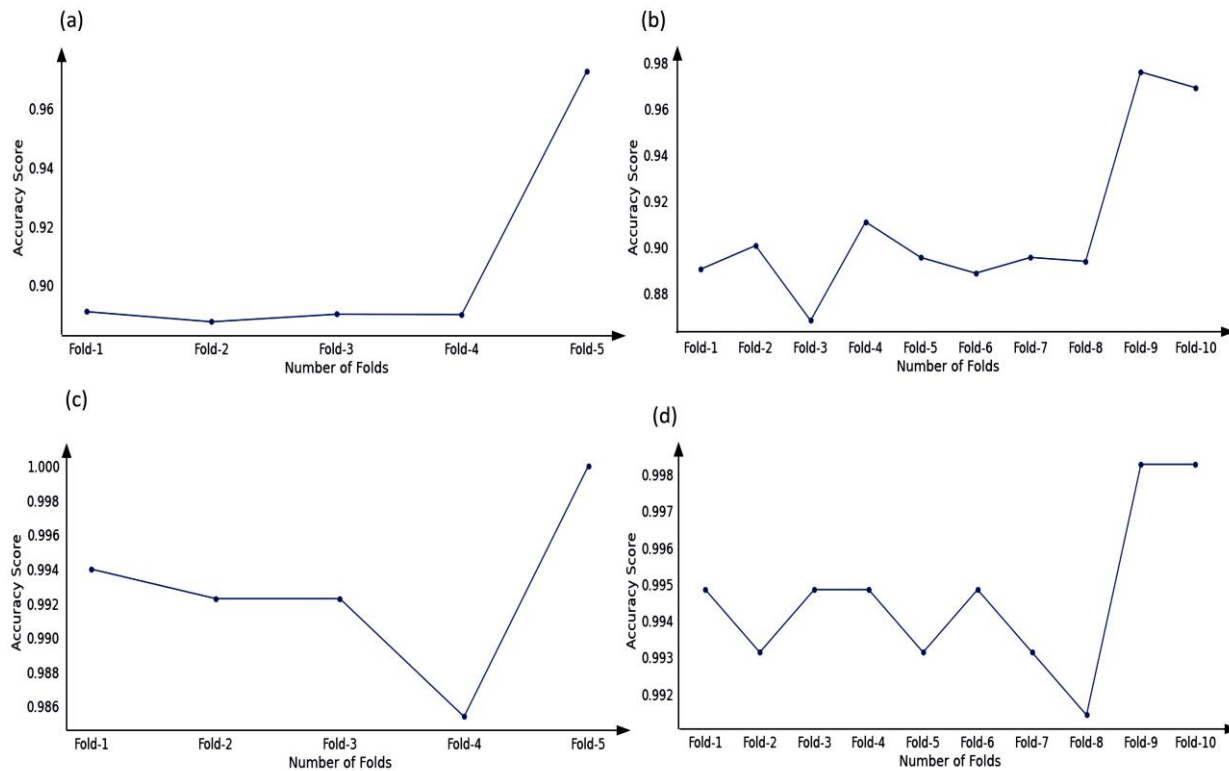


**Fig. 13** Accuracy plot while employing the Cross-Validation technique on the WARDIC classifier variants, *i.e.*, Superimposed on DenseNet-121 ConvNet with (a) 5-Fold Cross-Validation with the One-Class SVM classifier (b) 10-Fold Cross-Validation of One-Class SVM classifier (c) 5-Fold Cross-Validation with the Isolation Forest classifier (d) 10-Fold Cross-Validation with the Isolation Forest classifier.

based on various scores, *i.e.*, Accuracy (Acc), Precision, and Recall. Accuracy scores show an overall percentage of correctly identifying Explosive Weapons and Arms from the input images. The recall score measures the number of correct positive Small Arms results in all samples (positive samples). Precision shows the ratio of the actual Small Arms negatives to the correctly predicted. Our proposed performance evaluation assesses the WARDIC variants based on accuracy as WARDIC is a singular class classifier. Only True positive (TP) and False Negative (FN) exist in one-class classification problems as the data consists of only one class. Hence, True Negative (TN) and False positive (FP) is reduced to zero, resulting in equal accuracy and Recall and precision equalling unity. Formulas 3 and 4 measure accuracy and precision, important criteria for model evaluation.

$$A_{cc} = \frac{TP+TN}{TP+TN+FP+FN} \approx \frac{TP}{TP+FN} \quad (3)$$

$$Precision = \frac{TP}{TP+FP} \approx \frac{TP}{TP+0} = 1 \quad (4)$$

(Abbreviations: TP- True Positive, TN- True Negative, FP- False Positive, FN- False Negative)

#### 4.2 Quantitative results

The section covers the detailed discussion on the evaluation of the WARDIC experiments where we augmented the One-class SVM and Isolation Forest classifiers with ConvNet models,

*i.e.*, VGG19, VGG16, MobileNetV2, MobileNet, InceptionV3, InceptionResNetV2, DenseNet121, EfficientNetB0, EfficientNetB1 and, NASNetMobile followed a summarised comparative study. The section presents results for baseline models, tuned models, and cross-validation. It shows the results as 'Baseline Accuracy' while the classifier predicts while initialized with the random state. Deliberate experiments improved the results by tuning the proposed set of variants/hyperparameters while employing the Singular classifier. We have not changed any layers in the ConvNet models while extracting features. We evaluated the augmented model and showed the performance as 'Obtained Accuracy.' In experiments, the DenseNet121 fused with the Singular classifier gave benchmarking results. We used ReLu as an activation function in the ConvNet. While using OCSVM, we used Gamma= 0.001, Kernel='rbf', and Nu=0.08. We used Isolation Forest with contamination=0.08, max\_features=1.0, max\_samples=1.0, n\_estimators=40, and random\_state=42. We also present the results of the cross-validation experiments, where we employed the k-fold cross-validations with k=5 and 10. Table 3 shows the comparative analysis of the ConvNet models' augmentation experiments with the One-class SVM and Isolation Forest Classifier. Table 4 shows the performance criteria with a comparative analysis of all the experimented ConvNet models' augmentation with the Isolation Forest Classifier.

**Table 3.** The table illustrates the results of the implemented fused models, *i.e.*, Feature Extraction Using ConvNets, namely VGG16, VGG-19, MobileNet, MobileNetV2, InceptionResNetV2, DenseNet121, EfficientNet B0, EfficientNet B1, and NASNetMobile and Classification algorithm using One-Class SVM and Isolation Forest. The evaluation criteria/ performance metrics for Weapons and Arms detection with Singular Classifier are shown along with their 5-fold and 10-fold cross-validation/predictions.

Feature ConvNet	Extraction	Classification Algo	Baseline Acc%	Obtained Acc%	5-Fold CV Acc %	10-Fold CV Acc%
VGG-16		OCSVM	0.6843	0.9828	0.9052	0.9777
		IF	0.9991	0.9991	0.9777	0.9802
VGG-19		OCSVM	0.674	0.9794	0.9032	0.9075
		IF	0.9974	0.9974	0.9746	0.9756
MobileNet		OCSVM	0.7607	0.9931	0.9052	0.9085
		IF	1	1	0.9922	0.9903
MobileNet V2		OCSVM	0.7006	0.9888	0.8974	0.9013
		IF	0.9991	1	0.9617	0.966
Inception ResNetV2		OCSVM	0.5385	0.9313	0.9071	0.9087
		IF	0.9674	0.9682	0.9416	0.9430
DenseNet121		OCSVM	0.7118	0.9725	0.9063	0.9087
		IF	0.9991	1	0.9927	0.9946
EfficientNetB0		OCSVM	0.644	0.9708	0.9023	0.9049
		IF	0.9897	0.9922	0.9622	0.9617
EfficientNetB1		OCSVM	0.6312	0.9682	0.9034	0.9053
		IF	0.9897	0.9922	0.9659	0.9639
NASNetMobile		OCSVM	0.6243	0.9682	0.9025	0.9053
		IF	0.9862	0.9888	0.9469	0.9480

**Table 4.** The table illustrates the results of the implemented fused models, *i.e.*, Feature Extraction Using ConvNets, namely VGG16, VGG-19, MobileNet, MobileNetV2, InceptionResNetV2, DenseNet121, EfficientNet B0, EfficientNet B1, and NASNetMobile and Classification algorithm using Isolation Forest Classifier. The evaluation criteria/ performance metrics for Weapons and Arms detection with Singular Classifier are shown along with their obtained accuracy, 5-fold CV accuracy, Precision, Recall, F1-Score, and Parametres (while using ConvNets for feature extraction).

ConvNet	Obtained Acc	5-Fold CV Acc	Prec	Recall	F1-Score	Params
VGG-16	0.9991	0.9777	1.0	0.97	0.98	14,714,688
VGG-19	0.9974	0.9746	1.0	0.98	0.99	20,024,384
MobileNet	1	0.9922	1.0	0.98	0.99	3,228,864
MobileNet V2	1	0.9617	1.0	0.99	0.99	2,257,984
Inception ResNetV2	0.9682	0.9416	1.0	0.96	0.98	54,336,736
DenseNet121	1	0.9927	1.0	0.98	0.99	7,037,504
EfficientNetB0	0.9922	0.9622	1.0	0.98	0.99	4,049,571
EfficientNetB1	0.9922	0.9659	1.0	0.98	0.99	6,575,239
NASNetMobile	0.9888	0.9469	1.0	0.98	0.99	4,269,716

The OCSVM classifier showed significant performance improvement, as distinctly highlighted by the baseline and optimized model plots. The confusion matrix shown in Fig. 14 illustrates the performance of the baseline and optimized model, *i.e.* (DenseNet121 ConvNet + Isolation Forest). The section highlights the results attained by the WARDIC classifier (DenseNet121 ConvNet + Isolation Forest). It shows a significant drop in False positives prediction of samples post tuning of significant parameters, thus improving the accuracy

significantly. The graphs show the least degree of deviation supporting the results presented in Table 3. The experiments achieved a perfect unit accuracy score while fusing MobileNetV2, MobileNet, and DenseNet121 with the Isolation Forest Classifier. The Isolation Forest classifier demonstrated a symmetric performance trend over the baseline and optimized models with marginal but promising performance. The entire optimized combination is referred as - 'WARDIC', the best performing augmentation. The Cross-

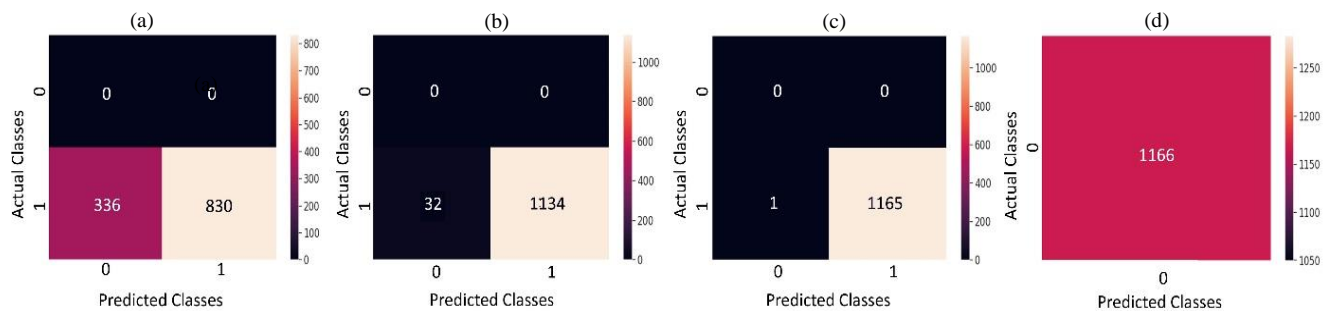


**Fig. 14** Classification predictions of the classification by WARDIC variant models (using DenseNet121 ConvNet feature extraction) with (a) Baseline One-Class SVM classifier, (b) Optimized One-Class SVM classifier, (c) Baseline Isolation Forest classifier, (d) Optimized Isolation Forest classifier.

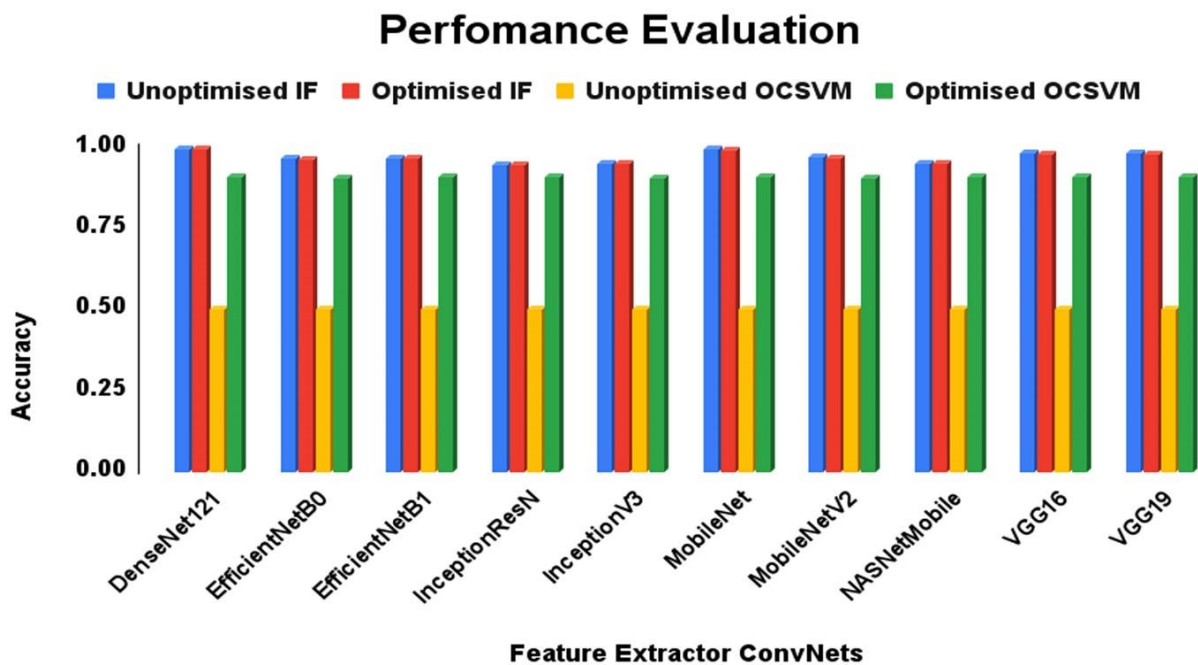


**Fig. 15** Comparative performance of experimented variants, *i.e.*, ConvNet models with the Singular Classifiers, *i.e.*, One class SVM classifier, Isolation Forest classifier. The graphs highlight the performance of unoptimized viz-a-viz of the cross-validated optimized (5-Fold/10-Fold) WARDIC model variants.

validation graph plot of the WARDIC of the Mean 5-fold and 10-Fold is shown in Fig. 15. The models with the highest performance scores were evaluated by obtaining the Floating-point operations per second or FLOPS on Tesla T4 GPU. DenseNet121, MobileNet, EfficientNetB0, and VGG-16 augmented with Isolation Classifier accomplished calculations in 0.0178, 0.3926, 3.1715, and 0.141 BLOPS respectively. DenseNet121 + Isolation Forest consumed the least resources, *i.e.*, 0.0142 GB GPU with 26.84 MB Memory for model weights, proving better suited for the referenced scenario being the most light-weighted Model.

**5. Conclusion and future work**

The research aims to address the real challenges various Law enforcement agencies face worldwide. The methodology proposes a novel weapon identification pipeline by analyzing the surveillance video/ image feeds that spot explosive

weapons and arms. First, a highly relevant, balanced dataset of images encountered in the operation scenario by the Armed Forces and Law enforcement agencies- referred to as NOWAD with 50+ different explosive weapons and small arms with considerable chromatic exposure- is introduced. This phase deliberated on relevancy and diversity of images by deliberate EDA on NOWAD. The WARDIC classifier is a novel approach by fusing State-of-the-Art CNN with an Isolation Forest algorithm. The experiments enhanced results using the transfer learning technique, which enhanced the new tasks' learning and enabled improved feature extraction. The proposed pipeline starts with features extraction dovetailed by singular classifiers to recognize the weapons. The experiments attained a perfect unit accuracy score while fusing MobileNetV2, MobileNet, and DenseNet121 with the Isolation Forest Classifier. Results highlight the evaluation and performance scores attained by the WARDIC classifier,

i.e., the fusion of tuned DenseNet121 ConvNet + Isolation Forest classifier with the accuracy score of a unity. The performance was cross-validated using the 5-Fold and 10-Fold techniques by attaining mean accuracy scores of 99.27% and 99.46%, respectively. The NOWAD dataset and WARDIC enable the State-of-the-Art Classifier formulation, shortening the OODA loop for effective decision-making, thus enabling a quick response system. The commanders on the ground get empowered by employing the proposed methodology, ensuring faster results with high compatibility to ride on low computation infrastructure. Future work entails amalgamating the NOWAD with multi-class images about the scenario and conducting multi-class classification experiments. The experiments are subjected to practical time complexity to achieve optimum performance, aiding military and law-enforcement agencies in effective operations' conduct.

### Acknowledgements

We want to convey gratitude to Provost, Registrar, CHARUSAT, Changa, India, for the support during this work, without which the outcome would not have been possible. We also thank Simranjit Singh for technical assistance during the dataset creation/ evaluation and graphical exploration.

### Conflict of Interest

The authors declare no conflict of interest.

### Supporting information

Not applicable.

### References

- [1] U. N. UN, silence the guns urges un disarmament chief as global week of action begins, <https://news.un.org/en/story/2018/05/1009082>, May 2018.
- [2] R. Peters, Small arms: No single solution, *UN Chronicle*, 2012, **46**, 61-65, doi: 10.18356/e618f617-en.
- [3] C. Redcross, explosive weapons in populated areas humanitarian, legal, technical and military aspects, [https://www.icrc.org/en/download/file/13231/icrc\\_ewpa\\_report\\_12.06.20151.pdf](https://www.icrc.org/en/download/file/13231/icrc_ewpa_report_12.06.20151.pdf), Feb. 2015.
- [4] F. P. P. Staff, July 2017. Available: <https://www.firstpost.com/photos/india-gallery/stone-pelters-of-kashmir-heres-a-look-at-those-behind-masks-3793905.html>.
- [5] H. S. R. C. Steven Gordon, What research tells us is driving xenophobic attacks on african migrants in south africa, September 2019, Available: <https://qz.com/africa/1705349/how-south-africa-xenophobia-attacks-on-africans-is-driven/>.
- [6] E. Rojas-Sasse, South america's protests fueled by 'extreme' social inequality, October 2019, Available: <https://p.dw.com/p/3Rtao>.
- [7] N. Cassandra Vinograd, Iraqis vote in critical elections amid upsurge in violence, April 2014, Available: <https://www.nbcnews.com/news/world/>.
- [8] N. Press, Gen gatkouth takes akoka, oil fields vacated as workers flee!, February 2014, Available: <https://nyamile.co/2014/02/22/gen-gatkouth-takes-akoka-oil-fields-vacated-as-workers-flee/>.
- [9] O. M. Associated Press, Yemen rebels claim attack on saudi oil facility in jeddah, November 2019, Available: <https://www.outlookindia.com/website/story/world-news-yemen-rebels-claim-attack-on-saudi-oil-facility-in-jeddah/365124>.
- [10] W. S. Angerman, Coming full circle with boyd's ooda loop ideas: An analysis of innovation diffusion and evolution, 2004.
- [11] B. Brehmer, The dynamic ooda loop: Amalgamating boyd's ooda loop and the dynamic decision loop, 2005.
- [12] D. K. J. E. von Lubitz, J. E. Beakley, F. Patricelli, 'All hazards approach' to disaster management: the role of information and knowledge management, Boyd's OODA Loop, and network-centricity, *Disasters*, 2008, **32**, 561-585, doi: 10.1111/j.1467-7717.2008.01055.x.
- [13] J. Boyd, G. T. Hammond, A discourse on winning and losing. Maxwell AFB, Alabama: *Air University Press*, Curtis E. LeMay Center for Doctrine Development and Education, 2018.
- [14] N. Vallez, A. Velasco-Mata, O. Deniz, Deep autoencoder for false positive reduction in handgun detection, *Neural Computing and Applications*, 2021, **33**, 5885-5895, doi: 10.1007/s00521-020-05365-w.
- [15] M. T. Bhatti, M. G. Khan, M. Aslam, M. J. Fiaz, Weapon detection in real-time CCTV videos using deep learning, *IEEE Access*, 2021, **9**, 34366-34382, doi: 10.1109/access.2021.3059170.
- [16] N. Dwivedi, D. K. Singh, D. S. Kushwaha, Weapon classification using deep convolutional neural network. *2019 IEEE Conference on Information and Communication Technology*. December 6-8, 2019, Allahabad, India. IEEE, 2020, 1-5, doi: 10.1109/CICT48419.2019.9066227.
- [17] H. Jain, A. Vikram, Mohana, A. Kashyap, A. Jain, Weapon detection using artificial intelligence and deep learning for security applications. *2020 International Conference on Electronics and Sustainable Communication Systems (ICESC)*. July 2-4, 2020, Coimbatore, India. IEEE, 2020, 193-198, doi: 10.1109/ICESC48915.2020.9155832.
- [18] J. Lai, S. Maples, Developing a real-time gun detection classifier, *Course: CS231n, Stanford University*, 2017.
- [19] S. Narejo, B. Pandey, D. Esenarro vargas, C. Rodriguez, M. R. Anjum, Weapon detection using YOLO V3 for smart surveillance system, *Mathematical Problems in Engineering*, 2021, **2021**, 1-9, doi: 10.1155/2021/9975700.
- [20] R. F. A. Kanehisa, A. A. Neto, Firearm detection using convolutional neural networks, *ICAART (2)*, 2019, 707-714, doi: 10.5220/0007397707070714.
- [21] R. Olmos, S. Tabik, F. Herrera, Automatic handgun detection alarm in videos using deep learning, *Neurocomputing*, 2018, **275**, 66-72, doi: 10.1016/j.neucom.2017.05.012.
- [22] G. K. Verma, A. Dhillon, A Handheld Gun Detection using Faster R-CNN Deep Learning, *Proceedings of the 7th International Conference on Computer and Communication Technology - ICCCT-2017*. November 24-26, 2017. Allahabad, India. New York: ACM Press, 2017: 84-88, doi:

- 10.1145/3154979.3154988.
- [23] J. Ruiz-Santaquiteria, A. Velasco-Mata, N. Vallez, G. Bueno, J. A. Alvarez-Garcia, O. Deniz, Handgun detection using combined human pose and weapon appearance, *IEEE Access*, 2021, **9**, 123815-123826, doi: 10.1109/access.2021.3110335.
- [24] A. Carlier, Openlabeling++, <https://github.com/alexandre01/OpenLabeling>, 2019.
- [25] A. Krizhevsky, I. Sutskever, G. E. Hinton, ImageNet classification with deep convolutional neural networks, *Proceedings of the 25th International Conference on Neural Information Processing Systems - Volume 1*. December 3 - 6, 2012, Lake Tahoe, Nevada. New York: ACM, 2012, 1097-1105, doi: 10.5555/2999134.2999257.
- [26] A. Krizhevsky, I. Sutskever, G. E. Hinton, ImageNet classification with deep convolutional neural networks, *Communications of the ACM*, 2017, **60**, 84-90, doi: 10.1145/3065386.
- [27] H. Abdi, L. J. Williams, Principal component analysis, *Wiley Interdisciplinary Reviews: Computational Statistics*, 2010, **2**, 433-459, doi: 10.1002/wics.101.
- [28] K. Simonyan, A. Zisserman, Very deep convolutional networks for large-scale image recognition, *arXiv preprint arXiv:1409.1556*, 2014, <https://arxiv.org/abs/1409.1556>.
- [29] M. Sandler, A. Howard, M. Zhu, A. Zhmoginov, L.-C. Chen, MobileNetV2: inverted residuals and linear bottlenecks. *2018 IEEE/CVF Conference on Computer Vision and Pattern Recognition*. June 18-23, 2018, Salt Lake City, UT, USA. IEEE, 2018, 4510-4520, doi: 10.1109/CVPR.2018.00474.
- [30] A. G. Howard, Menglong Zhu, Bo Chen, D. Kalenichenko, Weijun Wang, T. Weyand, M. Andreetto, H. Adam, MobileNets: efficient convolutional neural networks for mobile vision applications, *arXiv preprint arXiv:1704.04861*, 2017, <https://arxiv.org/abs/1704.04861>
- [31] C. Szegedy, V. Vanhoucke, S. Ioffe, J. Shlens, Z. Wojna, Rethinking the inception architecture for computer vision. *2016 IEEE Conference on Computer Vision and Pattern Recognition (CVPR)*. June 27-30, 2016, Las Vegas, NV, USA. IEEE, 2016, 2818-2826, doi: 10.1109/CVPR.2016.308.
- [32] G. Huang, Z. Liu, L. van der Maaten, K. Q. Weinberger, Densely connected convolutional networks. *2017 IEEE Conference on Computer Vision and Pattern Recognition (CVPR)*. July 21-26, 2017, Honolulu, HI, USA. IEEE, 2017, 2261-2269, doi: 10.1109/CVPR.2017.243.
- [33] M. Tan, Q. Le, EfficientNet: rethinking model scaling for convolutional neural networks, *International conference on machine learning*, 2019, 6105-6114, <https://arxiv.org/abs/1905.11946>
- [34] B. Zoph, V. Vasudevan, J. Shlens, Q. V. Le, Learning transferable architectures for scalable image recognition. *2018 IEEE/CVF Conference on Computer Vision and Pattern Recognition*. June 18-23, 2018, Salt Lake City, UT, USA. IEEE, 2018, 8697-8710, doi: 10.1109/CVPR.2018.00907.
- [35] S. J. Pan, Q. Yang, A survey on transfer learning, *IEEE Transactions on Knowledge and Data Engineering*, 2010, **22**, 1345-1359, doi: 10.1109/TKDE.2009.191.
- [36] A. R. Bhatt, A. Ganatra, K. Kotecha, Cervical cancer detection in pap smear whole slide images using convNet with transfer learning and progressive resizing, *PeerJ Computer Science*, 2021, **7**, e348, doi: 10.7717/peerj-cs.348.
- [37] A. Bhatt, A. Ganatra, K. Kotecha, COVID-19 pulmonary consolidations detection in chest X-ray using progressive resizing and transfer learning techniques, *Heliyon*, 2021, **7**, e07211, doi: 10.1016/j.heliyon.2021.e07211.
- [38] P. Perera, V. M. Patel, Learning deep features for one-class classification, *IEEE Transactions on Image Processing*, 2019, **28**, 5450-5463, doi: 10.1109/tip.2019.2917862.
- [39] S. S. Khan, M. G. Madden, A survey of recent trends in one class classification, *Irish conference on artificial intelligence and cognitive science*, 2010, 188-197, doi: 10.1007/978-3-642-17080-5\_21.
- [40] B. Krawczyk, M. Woźniak, B. Cyganek, Clustering-based ensembles for one-class classification, *Information Sciences*, 2014, **264**, 182-195, doi: 10.1016/j.ins.2013.12.019.
- [41] L. Manevitz, M. Yousef, One-class SVMs for document classification, *Journal of Machine Learning Research*, 2002, **2**, 139-154.
- [42] S. S. Khan, M. G. Madden, One-class classification: taxonomy of study and review of techniques, *The Knowledge Engineering Review*, 2014, **29**, 345-374, doi: 10.1017/s026988891300043x.
- [43] F. T. Liu, K. M. Ting, Z.-H. Zhou, Isolation forest. *2008 Eighth IEEE International Conference on Data Mining*. December 15-19, 2008, Pisa, Italy. IEEE, 2009, 413-422, doi: 10.1109/ICDM.2008.17.

**Publisher's Note:** Engineered Science Publisher remains neutral with regard to jurisdictional claims in published maps and institutional affiliations.